Andreas EILENBERGER, Manfred SCHROEDL

Technical University of Vienna

Extended Back EMF model for permanent magnet synchronous machine with different inductances in d- and q-axis

Abstract. *This paper discusses a reluctance-dependent back electromotive force (EMF) model for encoderless vector driven permanent magnet synchronous machines (PMSM) compared to well known, non reluctance-dependent back EMF models. Established PMSM could have considerable varieties in direct and quadrature inductances. So it makes sense to consider this behaviour in an extended back EMF model. On closer examination it will turn out that a reluctance dependent EMF model has a better behaviour at low speed as the standard model. Also the derivation of the extended model will be illustrated. Furthermore some simulation results and practical measurements will be discussed.*

Streszczenie. *W artykule przedstawiono wpływ zależnej od reluktancji siły elektromotorycznej (EMF) dla bezczujnikowego sterowania maszyny synchronicznej z magnesami trwałymi (PMSM) w porównaniu z powszechnie znanym modelem nie uwzględniającym tego wpływu. Założony model PMSM może mieć różne warianty. Z tego powodu rozważono zachowanie układu z rozszerzonym modelem siły elektromotorycznej EFM. Z badań wynika, że model zależnej od reluktancji siły elektromotorycznej ma lepsze właściwości przy małych prędkościach obrotowych niż model standardowy. Pokazano wyprowadzenie zależności modelu rozszerzonego. Przedstawiono także wybrane wyniki badań symulacyjnych i laboratoryjnych. (**Rozszerzony model EMF dla maszyny synchronicznej z magnesami trwałymi z różnymi indukcyjnościami w osiach d- i q**)*

Keywords: Electrical Drive, Permanent magnet motor, Synchronous motor, Reluctance drive, Sensorless control.
Słowa kluczowe: napęd elektryczny, silnik z magnesami trwałymi, silnik synchroniczny, napęd reluktancyjny, sterowanie bezczujnikowe.

Introduction

There are a lot of publications on the field of sensorless driven PMSM, which means replacing the mechanical position encoder by mathematical models. Low speed models combined with a back EMF model for higher speed enables an operation in the whole speed range. The lower the speed the more sensitive the parameters of the EMF model are. Such parameters are stator inductance and stator resistance. In most cases there is a significant difference between direct and quadrature inductance. Hence, this paper describes an extended EMF model with regard to the saliency to achieve highly dynamical operation in a wide speed range, especially at low speed.

The classical back EMF model

In the subsequent analyses for determining the operational behavior of the given machine, steady-state operation in conjunction with constant rotor angular velocity ω_K is supposed. All data are given in normalized values. The following calculations deal with the classical back EMF model [1], [2] and [6]. The stator flux linkage $\underline{\psi}_S$ is derived from the stator voltage equation

$$\underline{u}_S = r_S \cdot \underline{i}_S + \frac{d}{d\tau}\underline{\psi}_S + j\omega_K \underline{\psi}_S \tag{1}$$

by integration

$$\underline{\psi}_S(\tau) = \int \left[\underline{u}_S(\tau) - r_S \cdot \underline{i}_S(\tau)\right] d\tau \,.$$

Furthemore flux linkage $\underline{\psi}_m$ due to permanent magnets is calculated from stator flux linkage $\underline{\psi}_S$

$$\underline{\psi}_S = l_S \cdot \underline{i}_S + \underline{\psi}_m \tag{2}$$

and yields in the $\alpha\beta$ stator-oriented reference frame to equations

$$\psi_{m\alpha}(\tau) = \int \left[u_{s\alpha}(\tau) - r_S \cdot i_{S\alpha}(\tau)\right] d\tau - l_S \cdot i_{S\alpha}(\tau)$$
$$\psi_{m\beta}(\tau) = \int \left[u_{s\beta}(\tau) - r_S \cdot i_{S\beta}(\tau)\right] d\tau - l_S \cdot i_{S\beta}(\tau)$$

Normally, the integration is stabilized by a certain feedback. The argument of flux linkage vector ψ_m is the searched rotor position γ

$$\begin{aligned}\gamma &= \arg\left[\underline{\psi}_m\right] = \arctan\left[\frac{\psi_{m\beta}}{\psi_{m\alpha}}\right] = \\ &= \arctan\left\{\frac{\int\left[u_{s\alpha}(\tau) - r_S i_{S\alpha}(\tau)\right] d\tau - l_S i_{S\alpha}(\tau)}{\int\left[u_{s\beta}(\tau) - r_S i_{S\beta}(\tau)\right] d\tau - l_S i_{S\beta}(\tau)}\right\}\end{aligned} \tag{3}$$

Extended back EMF model

Using well known two-axis theory [4], [5] the flux linkage $\underline{\psi}_S$ in the dq rotor-oriented reference frame is given by

$$\underline{\psi}_{s,dq} = \underline{\psi}_{m,dq} + l_d i_d + j l_q i_q \qquad \Big|\cdot e^{j\gamma} \tag{4}$$

$$\underline{\psi}_{s,\alpha\beta} = \underline{\psi}_{m,\alpha\beta} + \left(l_d i_d + j l_q i_q\right)\cdot\left(\cos\gamma + j\sin\gamma\right)$$
$$\underline{\psi}_{s,\alpha\beta} = \underline{\psi}_{m,\alpha\beta} + l_d i_d \cos\gamma - l_q i_q \sin\gamma + j\left(l_q i_q \cos\gamma + l_d i_d \sin\gamma\right)$$

which yields to

$$\psi_{m\alpha} = \psi_{s\alpha} - l_d i_d \cos\gamma + l_q i_q \sin\gamma \tag{5}$$
$$\psi_{m\beta} = \psi_{s\beta} - l_d i_d \cos\gamma - l_q i_q \sin\gamma \tag{6}$$

The rotor position γ follows with simplified notation to

$$\arctan\left\{\frac{\int\left(u_\alpha - r_s i_\alpha\right) d\tau - l_d i_d \cos\gamma + l_q i_q \sin\gamma}{\int\left(u_\beta - r_s i_\beta\right) d\tau - l_d i_d \cos\gamma - l_q i_q \sin\gamma}\right\}. \tag{7}$$

The block diagram of the realized extended EMF model is shown in fig. 3. Furthermore an extended observer structure as discussed in [3] is implemented.

Experimental setup

For verification of the novel back EMF model, an outerrotor PMSM was used, shown in fig. 2. Furthermore a voltage source inverter with only a DC-link measurement is used. A short overview of the given hardware is shown in figure 1. The subsequent table 1 specifies the characteristics of the used PMSM.

Following fig. 2 shows the used outer-rotor PMSM with assembled encoder and belt to load-machine.

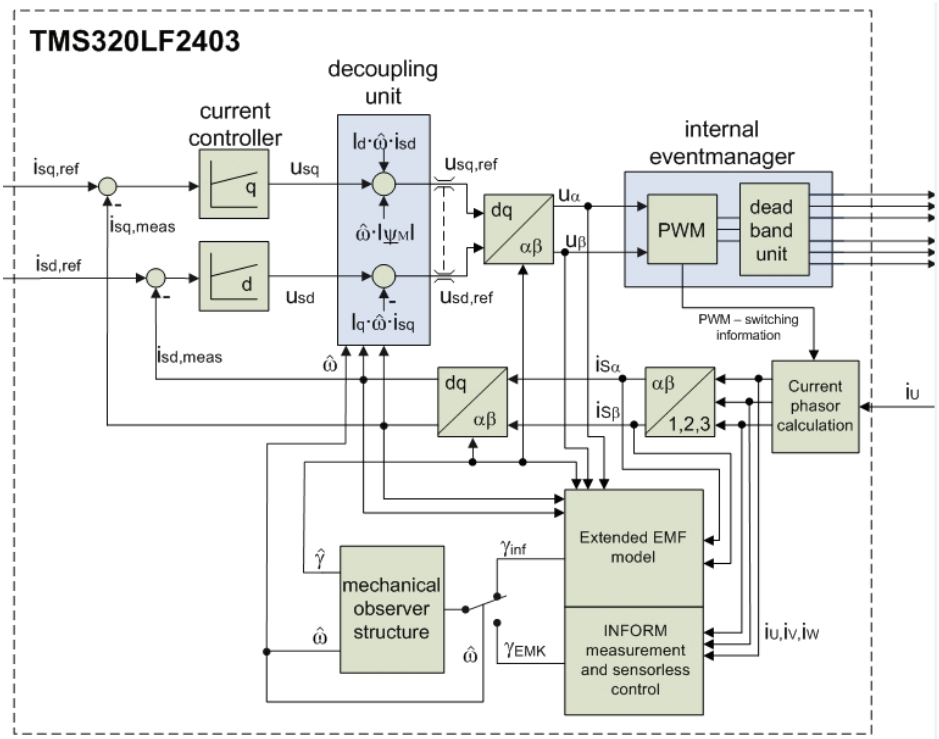

Fig. 1. Structure of the realized encoderless drive with an outer-rotor PMSM

Table 1. Characteristics of PMSM with outer rotor

continuous torque:	24 Nm
steady state current:	19 A rms
reference voltage level:	18.5 V
battery voltage:	46 V
rated output power:	750 W
rated velocity:	300 rpm
number of pole pairs:	p=12
stator resistance:	$r_s \approx 0.2$
direct inductance:	$l_d \approx 0.11$
quadrature inductance:	$l_q \approx 0.16$

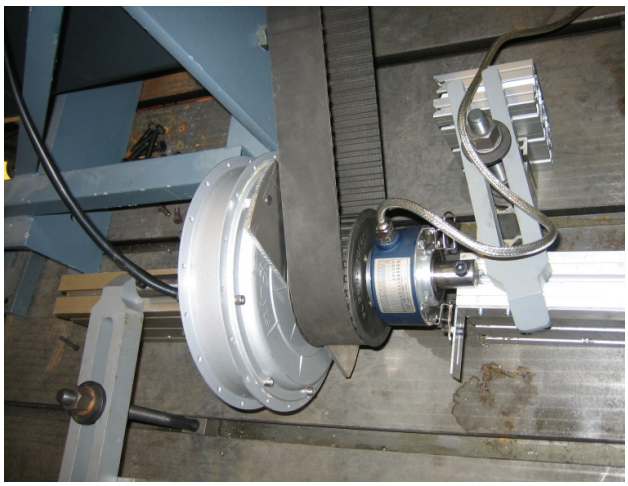

Fig.2. Picture of the used outer-rotor PMSM with encoder and load-machine

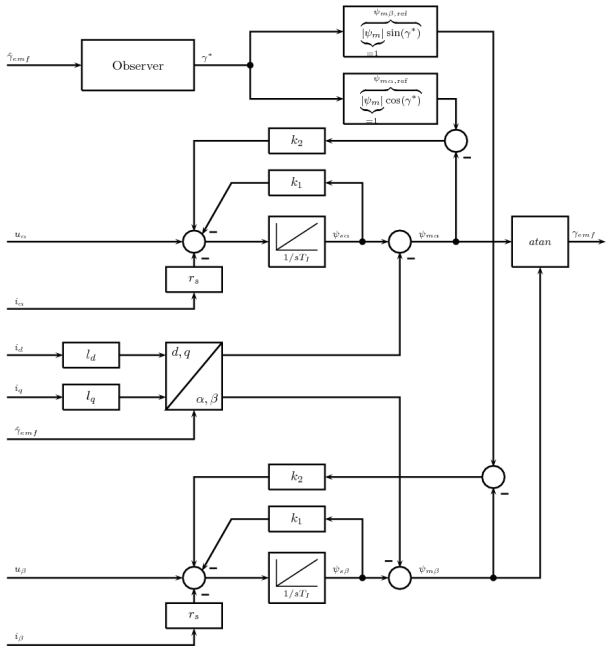

Fig. 3. Schematic of the realized extended back EMF model with extended observer structure [3]

Simulation results

For simulation of both back EMF models the simulation tool MATLAB-Simulink is used. In the following, two scenarios were simulated. First scenario shows results of the calculated rotor position with the well known EMF model with constant inductances and extended EMF model at constant quadrature-axis current $i_{q,ref.}$ To verify results, the reference rotor position is mapped. This simulation starts at standstill and accelerates rotor speed slowly. As be can seen in fig. 4 the extended back EMF model provides a useful angular rotor position at first while increasing the

rotor speed. At higher speed, the standard back EMF model also yields an angular rotor position. The significant offset between reference and calculated EMF angular rotor position is a result of the integrator feedback. An offset on voltage space phasor $u_{s\alpha}$ is used in the simulation representing voltage measurement errors of the experimental setup.

The second scenario shows the behaviour of the EMF models (fig. 5) at a constant rotor speed $\omega = 0.2$ with a rising quadrature current $i_{q,ref}$.

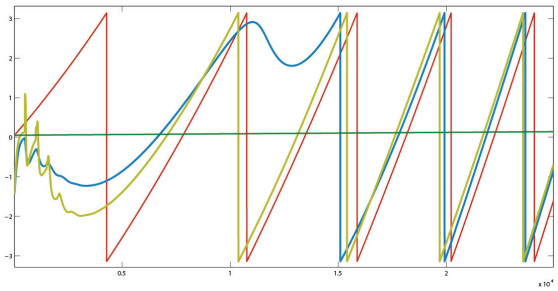

Fig. 4. Characteristics of calculated rotor position with standard back EMF model (blue) and extended back EMF model (yellow), furthermore encoder position (red) and rising rotor velocity (green) with $i_{q,ref}$ = 0.8.

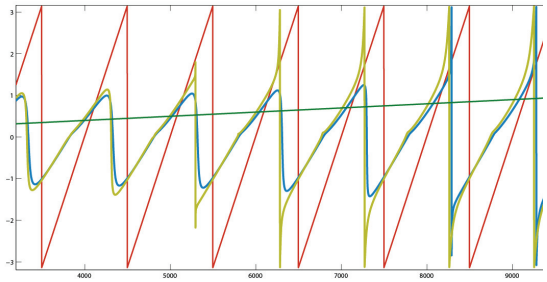

Rys. 5. Characteristics of calculated rotor position with standard back EMF model (blue) and extended back EMF model (yellow), encoder position (red) and the rising quadrature current $i_{q,ref}$ (green) with constant $\omega = 0.2$

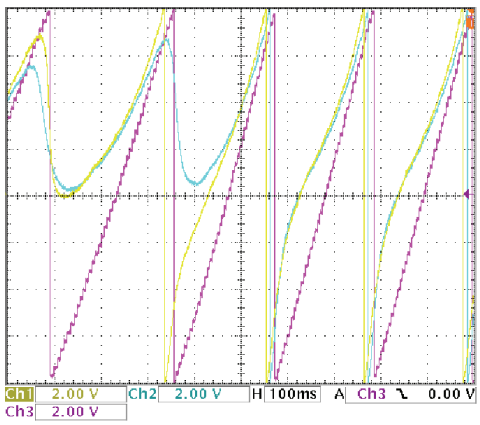

Rys. 6. Measured characteristics with a rising rotor speed and constant $i_{q,ref}$ = 0.5, Ch1: extended model (22.5/Div.), Ch2: novel model (22.5/Div.), Ch3: encoder position (22.5/Div.)

Measurements results

The measured results verify the results of the two simulated scenarios. First diagram (fig. 6) depicts the measurement according to fig. 4 with increasing rotor speed. Due to an offset error of the measured voltage space phasor $u_{s,\alpha\beta}$ the calculated rotor position with standard back EMF model has a visible positive offset.

Subsequent fig. 7 depicts the calculated angular rotor position with the mentioned two back EMF models at constant rotor speed and quadrature current. The extended model shows a better behaviour as the novel back EMF model.

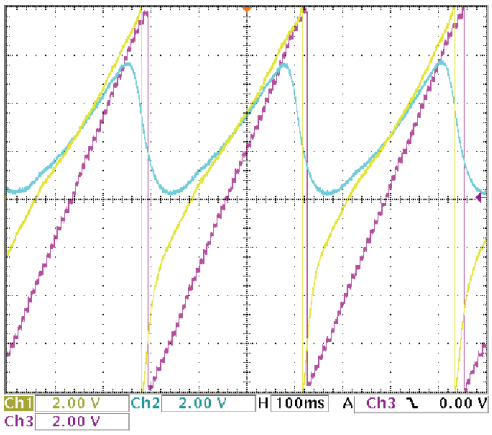

Fig. 7. Measured characteristics with $i_{q,ref}$ = 1 and ! _ 0.15, Ch1: extended model (22.5/Div.), Ch2: novel model (22.5/Div.), Ch3: encoder position (22.5/Div.)

Conclusion and outlook

This paper demonstrates an extended back EMF model with improved low-speed properties compared to the well known back EMF model with constant inductances, both with an observer structure. It is also shown that measured results with the experimental setup shows expected simulation results. Furthermore, the extended EMF model was successfully implemented in a drive for light vehicles.

The authors are very much indebted to the Austrian Science Foundation (FWF) which generously supports the work at the Institute of Electrical Drives and Machines at the Vienna University of Technology.

REFERENCES

[1] Schroedl M., Hofer M., Staffler W. "Combining INFORM method, Voltage model and mechanical observer for sensorless control of PM Synchronous Motors in the whole speed range including standstill", *PCIM, Nuernberg (Germany)*, (2006).
[2] Rieder U.-H.: "Optimierung der sensorlosen Regelung von permanentmagneterregten Aussenlaeufer-Synchronmaschinen", *PhD thesis*, Vienna University of Technology, 2005.
[3] Schroedl M., Hofer M., Staffler W. "Sensorless control of PM Synchronous Motors in the whole speed range including standstill using a combined INFORM/EMF model", *EPE-PEMC, Portoroz (Slovenia)*, (2006).
[4] Park R.H., "Two-Reaction Theory of synchronous machines, Generalized Method of Analysis", *AIEE Trans.*, pt. I, Vol.48, pp. 716, July 1929.
[5] Jones C. V., "The unified theory of electrical machines", *Butterworth & Co. (Publishers) Ltd.*,pt. II, London, 1967.
[6] T.M. Wolbank, M.A. Vogelsberger, R. Stumberger, "Adaptive Flux model for commissioning of signal injection based zero speed sensorless flux control of induction machines" *Proceedings of IEEE International Conference on Power Electronics and Drive Systems*, Bankok (2007)

Authors: *Dipl.-Ing. Andreas Eilenberger, Technical University of Vienna, Institute for Electrical Drives and Machines, Gusshausstrasse 25-29/E372, A-1040 Vienna, E-mail: andreas.eilenberger@ieam.tuwien.ac.at;*
Dipl.-Ing. Dr. Manfred Schroedl,
E-mail: manfred.schroedl@ieam.tuwien.ac.at